**EAI Endorsed Transactions**
**on Pervasive Health and Technology**
Research Article EAI.EU

# Automated Detection of fundus retinal image using EGODD algorithm

Subha K.[1, *] and S. Kother Mohideen[2]

[1]Sri Ram Nallamani Yadava College of Arts and Science, Tirunelveli, Tamil Nadu, India

[2]Sri Ram Nallamani Yadava College of Arts and Science, Tirunelveli, Tamil Nadu, India. Email: drskmkother@gmail.com

## Abstract

The developed device is tested for optical disc identification in the retinal image of the fundus. The theme chosen was interesting, as optical disc detection plays a critical role in retinal image processing for recognizing other fundus structures and is essential for identifying eye-related diseases. Because human visual vision has been little researched for optical disc detection and an effort to extract data analytics based on eye eyes, the proposed study first discovers how human perception functions for optical disc detection using a bottom-up visual focus paradigm. Eye-view data as the user conducts basic target-search tasks are obtained from separate user groups made up of experts and no expert groups. Extensive data processing has been carried out to extract eye gazing characteristics such as fixation and using computer approach mark regions in the fundus' retinal picture. Segregated labeled data was used to build up a piece of top-down information to bend the search map to the target area. The resulting Eye-based Optical Disk Detection System (EGODD) was tested through normal machine learning algorithms. This proposed framework has been tested and approved for optical disc detection; however, it can also be applied to other applications.

**Keywords:** Optic Disc Detection, Eye Fundus image, and machine learning techniques.

Received on 05 July 2021, accepted on 03 November 2022, published on 12 November 2022



doi: 10.4108/eetpht.v8i5.3170

## I. Introduction

The research goal was to understand how target detection can be achieved by incorporating the top-down (TD) approach, along with the bottom-up (BU) approach. This proposed study explains the study that uses eye monitoring for target detection, which aims to detect the target area using the information generated by domain experts' eye pattern. Image segmentation is an essential task in medical image processing, which is used to partition the image into several sectors with like characteristics using some predefined measurement criteria. In past decades several image segmentation has been proposed to improve the performance of segmentation. The segmentation goal is that the pixels in the same region have similar qualities, i.e., pixels from different regions have different qualities.

The study's key purpose is to propose a new prototype concept, the Eye Gaze-based Optical Disk Detection (EGODD) method. The technology's novelty has been confirmed through the scientific community and a patent with specification No. 201641037789. The title "Technology and process for identifying features in a picture using expert eye pattern information" has been filed. The goal of the research work was:

- To investigate how the bottom-up (BU) computational model works on fundus retinal images for OD detection.
- To investigate the behavioral difference between an expert and no expert groups by

*Corresponding author. Email: subhakandhi@gmail.com

studying their eye gaze patterns for the optic disc detection task.
- To develop a target detection system that integrates bottom-up (BU) and top-down (TD) approaches.

## II. Literature Survey

The study focuses on the awareness of the different fields where eye-tracking is used. The study and literature survey conducted here focuses on two key research fields: eye-tracking and optical disc identification. The fundamentals of each study field are clarified first, followed by a literature survey of this field.

A "Sparse Dissimilarity-constrained Coding for Glaucoma Screening," the system uses we propose a technique for the cup to Disc Ratio (CDR) evaluation utilizing 2D retinal fundus pictures [1].: In the proposed strategy, the optic circle is first sectioned and recreated [2]. Few methods based on fuzzy logic have been reported in the classification problems. The classifier's advancement is implemented to extract the fuzzy rules from the texture segmented regions of the HRCT images of lung cancer patients. An alternative kind called Fuzzy bean-based classifier, a supervised learning method with an appropriate optimization scheme propitious outcome, was accomplished [9]. Optimization was implemented in the obligatory parameters and differential evolution algorithm; hence, 73.9% classification accuracy is gained. Limited approaches based on the genetic algorithm have been stated. The genetic algorithm aids an innovative approach for advancing the semantic image segmentation system. Trials were established and estimated extensively on the benchmark data set for the segmentation of 21 objects. For estimating the right number of segments, an innovative technique was established for the automatic segmentation of human accustomed and anomalous images [10].

The upshot demonstrates that the proposed method has a noteworthy enhancement in image segmentation precision when related to comparable methods. The noise inhomogeneous physical regions are eradicated. Certain authors make use of both the Wiener and Anisotropic Diffusion Filters (ADF) in their research. Currently, the enhancement of lung structures of 3-D images is being implemented using numerous filters. Proposed the CAD system for radiologists analysis the lung nodule and improved the radiologist performance to detect the lung lesion with the time consuming and error-free process [11].

Even an experienced doctor will not be able to perform an accurate diagnosis with a single slice. Thus numerous successive slices were taken for precise diagnosis. Disparate the other traditional technique, which necessitates several slices to make an accurate assessment. A new technique has been proposed, demonstrating that effective Detection and diagnosis in just a single slice can be attained and is comparatively less time-consuming. The proposed method's key target is to enhance the accuracy and diminish the analysis time, false-positive reduction, and subjectivity to accurate segmentation of abnormal lung tissue with analysis of CT (Computed Tomography) scans.

Our proposed technique has additionally been tried for glaucoma screening. The technique accomplishes regions under the bend of 0.83 and 0.88 on datasets of 650 and 1676 pictures, separately, outflanking different strategies [3]. Right now, there is no powerful technique for minimal effort populace based glaucoma detection or screening.

"Optic cup segmentation from fundus images for glaucoma diagnosis," the proposed technique was assessed utilizing an open database for fundus pictures [4]. The test results exhibited that the proposed technique's cup limits were more predictable than existing strategies with ophthalmologists' outcomes. The proposed technique simultaneously exploited the two kinds of data, permitting it to remove precise cup limits both in zones with high shading contrasts and scanty vessels and in zones with little shading contrasts and swarmed vessels [5]. Within sight of a small number of mistaken shading data, focuses, or vessel twist focuses, the proposed strategy can, in any case, accomplish a precise optic cup limit.

"A Cloud-based system for Automatic Glaucoma Screening," we propose a half and half cloud arrangement that comprises of an open cloud level and private cloud level to address these worries [6]. This arrangement offers anyplace access in the open cloud level and stores delicate patients' data just as it performs a savvy evaluation of the disease in the private cloud level [8]. The pervasive anyplace get to nature of the framework through the cloud stage encourages more productive and savvy methods for glaucoma screening, permitting the sickness to be detected before and empowering early mediation for increasingly effective intercession and illness the board [7].

Assistant Technology (AT) is very useful for people with disabilities. Technology helps them perform activities that they have been unable to perform [12]. This would be extremely useful for most neuro-disabled patients. Face monitoring and a device will be used to pick a term from a menu. The keywords are chosen by the patient using eye-tracking strategies

[13]). These handheld devices are also useful for people with reduced hand functions. It can be built with various VR and virtual reality applications to recover and rehabilitate people with neuromata paralysis [14].

A new method of finding the optical disc in retinal images. Place of the optical disc and its core is the first phase of manufacturing [15]. Four retinal images are used to remove the histograms for each color variation. The average histogram in each colour is used to identify the middle of the optical disk.273 retinal photographs from the local datasets, DRIVE and STARE, are used throughout the work. The accuracy of the achieved rate is high [16].

The disease detection method using the optical disc boundary. Detection of macula position is known to be an aid of diabetic retinal examination. However, the drawback is that it would not include the general work of the anatomical form of the retinopathic images [17].

An aggressive contour and mathematical morphology strategy for detecting the border of OD in the retinal picture of the fundus. Pre-processing images using local minima detection and morphological filtering is performed to achieve correct boundary detection [20]. The OD boundary is defined using the active contour that is performed after pre-processing. This method has poor robustness but is effective in the analysis of large variable data.

The literature survey was performed to determine how eye-tracking applies to multiple technologies. Eye-tracking has played a key role in numerous technologies. The following chapter reflects on the fundamentals of the OD and the literature survey in the area of OD detection.

## 2.1 Contributions of the Proposed system

Following the objectives mentioned above, the targeted research contributions will be the following:

- The visual attention-based optic detection model was proposed to evaluate the user's search behavior while viewing disjunctive and conjunctive medical images. The need for top-down knowledge to be integrated was proved with performance analysis of optic disc detection using a bottom-up approach [18].
- The behavioral difference between an expert and no expert groups is investigated.
- An automated labeling system to distinguish target and non-target regions from eye gaze behavior of expert optometrists and non-expert groups while viewing fundus retinal images has been developed [19].
- Proposed a novel target detection system that combines bottom-up (BU) and top-down (TD) approaches.
- The proposed system has been evaluated on multiple datasets and across various models for its performance.

# III. Proposed system

The eye gaze-based optical disc detector (EGODD) method is tested for OD detector in retinal fundus images. However, the framework can also be applied to various target detection applications.

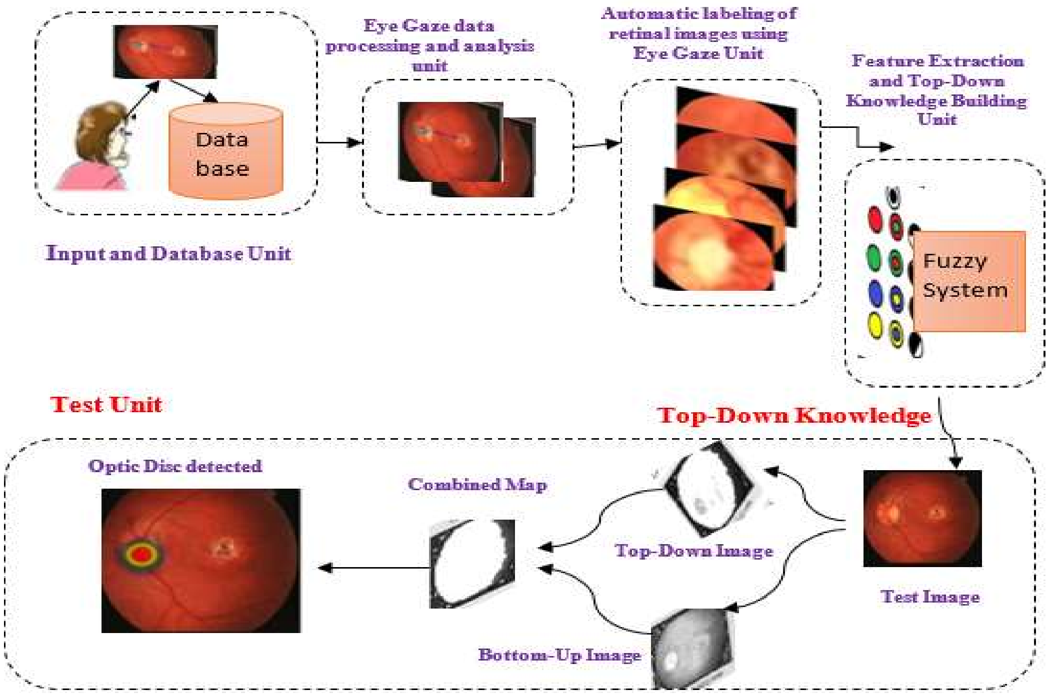


**Figure 3.1** Proposed system flow diagram

The fundus images may be divided into disjoint regions; histogram equalization is related to each region. Bilinear interpolation eliminates the boundary between the regions. The low contrast levels found out the small blood vessels.

$$\rho_n = 255\left(\frac{[\varphi_w(P) - \varphi_w(\min)]}{[\varphi_w(\max) - \varphi_w(\min)]}\right) \quad (3.1)$$

Where,

$$\varphi_w(\rho) = \left[1 + \exp\left(\frac{\mu_w - P}{\sigma_w}\right)\right]^{-1} \quad (3.2)$$

max, mins are the maximum and minimum intensity values of the fundus image.

$\mu_w$ is local window mean

$\sigma_w$ is standard deviation

$$\mu_w = \frac{1}{N^2} \sum_{(i,j)e(k,l)} P(i,j) \quad (3.3)$$

$$\sigma_w = \sqrt{\frac{1}{N^2} \sum_{(i,j)e(k,l)} ((P(i,j) - \mu_w))^2}$$

(3.4)

The pixel is adapted by using Equation (3.10)

$$I(x,y) = \left[\frac{1}{h^2} \sum_{q \in N_p} \partial\{I_p - I_q\}\right]^r * 255$$

(3.5)

Where δ(x) is a delta function

The contrast between vessels and the background becomes larger when the pixel value r increases. In the background, the noises are also improved, and the boundaries of some vessels are distorted. When h is small, the adaptive histogram equalization is improved, and the local information results in noise. When h is large, the results are smoother.

Vessel removal means removing the vessels. In this method, from the input image, the unwanted vessels are removed.

$$S = \sum_{i=1}^{12} \left(S_{op} - \gamma L_i(S_o)\right) \tag{3.6}$$

After extrapolation, this scheme is used to remove the uneven illuminations according to the following formula for each pixel intensity.

$$f_n = f_o + \mu_d - \mu_l \tag{3.7}$$

where

$f_n$ is the new pixel intensity value, and $f_o$ is the original pixel intensity value.

$\mu_d$ is the desired average intensity, and $\mu_l$ is the local average intensity.

In the proposed research, the localization phase includes the estimation of optic disc location. The principal component analysis method is used to identify the proper optic disc location PCA method include three steps

- In the training image, the Eigenvectors are computed.
- The fundus image is placed in the space specified by Eigenvectors.
- Compute the distance between the fundus image and projection

In the proposed research, the training set contains the fundus images. The optic disc is cropped from the training set. Sub images of intensity are normalized and resized by L*L pixels. $L^2$ is the vector dimension in the training set of the images.

The average vector of the training set is calculated by

$$\Psi = \frac{1}{M} \sum_{i=1}^{m} T_i \tag{3.8}$$

The average vector of the training set is

$$C = \frac{1}{M} \sum_{i=1}^{m} T_i \; \varphi_i \varphi_i^{\,T} = WW^T \tag{3.9}$$

where W is a matrix

$\varphi_i$ is the mean-centered value of the eye image.

In PCA, a set of images are required for training images. Let N be the total number of images used in the training image with n*n dimensions.

Let $mn_i$ and $mx_i$ are the minimum and maximum values in the training image set as follows

$$mn_i = min[I_i] \tag{3.10}$$

$$mx_i = max[I_i - mn_i] \tag{3.11}$$

The normalized training image is as follows

$$I_i^n = \frac{I_i - mn_i}{mx_i} 255 \tag{3.12}$$

In the training image, the mean is computed by the following Equation

$$M = \frac{1}{N} \sum_{i=1}^{N} I_i^{\,n} \tag{3.13}$$

The mean image is subtracted from the normalized training image as shown below

$$I_i^{nm} = I_i^n - m \tag{3.14}$$

The matrix can be written as,

$$\begin{pmatrix} I_i^{nm}[1,1] & \ldots\ldots\ldots\ldots & I_1^{nm}[1,n] \\ I_i^{nm}[2,1] & \ldots\ldots\ldots\ldots & I_1^{nm}[2,n] \\ I_i^{nm}[n,1] & \ldots\ldots\ldots & I_1^{nm}[n,n] \end{pmatrix}$$

The following equations give the required data formed by PCA

$$D = \left\{\{fI_i^{nm}[K, I]\forall 1 \leq i \leq N\}[2, N], I_i^{nm}[n, n]\right\} \quad (3.15)$$

The data D has a dimension, and the covariance matrix is formed by

$$C = \frac{D^T D}{N} \quad (3.16)$$

A feature vector is formed by

Feat vect = eigenvalue [c]

Feat vect is computed by $Finaldat_1$ and $\mathrm{sum}_1$ and is given by

$$Finaldat_1 = \mathrm{Feavec.}\, D^T$$

$$\mathrm{Sum}_1 = \sum_{p=1}^{N}\sum_{q=1}^{n_2} {Finaldat_1}^2[p, q] \quad (3.17)$$

The error is defined by

$$\mathrm{error} = \mathrm{Sum}_1 - \mathrm{Sum}_2 \quad (3.18)$$

The $sum_2$ is defined by

$$\mathrm{Sum}_2 = \sum_{p=1}^{N}\sum_{q=1}^{n_2} {Finaldat_2}^2[p, q] \quad (3.19)$$

The $Finaldat_2$is defined by

$$\mathrm{Finaldat}_2 = (\mathrm{Featvec}[1]^T.\{\mathrm{patch}\})$$

This method explains the training images and helps determine the similarity between the unknown image and the training set's image.

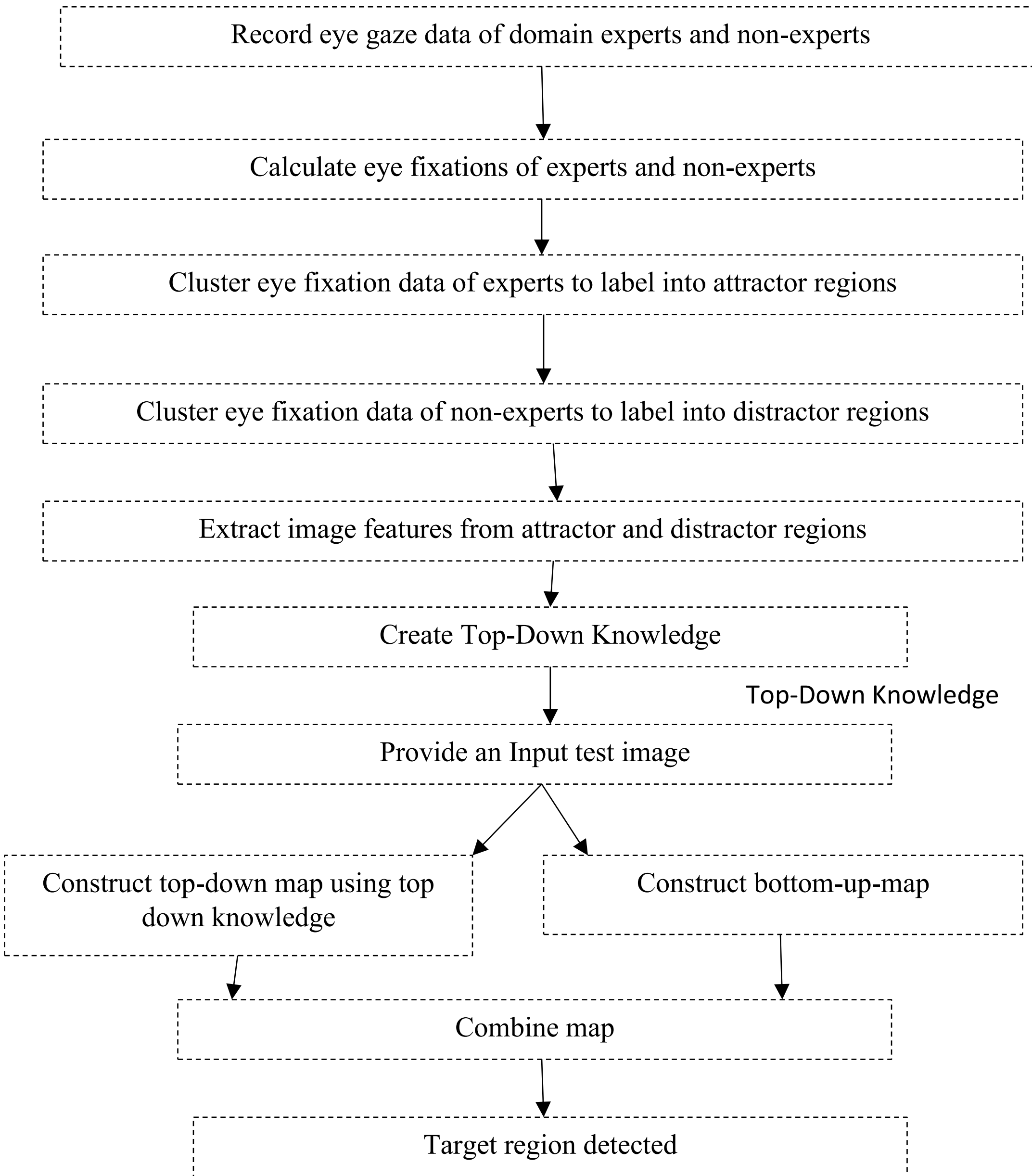


**Figure 3.2** Major steps in the eye gaze-based optic disc detection (EGODD) system.

## IV. Result and Discussion

DDSM is a database of scanned screen eye learning. There are about 2500 cases in the database. Each case of the right and left eye involves two image vision anatomies, such as CC and MLO. We have taken a total of 589 mammograms in our trial, including 331 benign and 258 malignant images. The planned method was experienced in the group of eye images and showed an important development in classification performance. Image patches can be extracted to train the network; finally, we classify an image as input. The performance of the network is superior to compare previous

classification algorithms for classifying an image.
The sample of images is shown in Fig .4.1

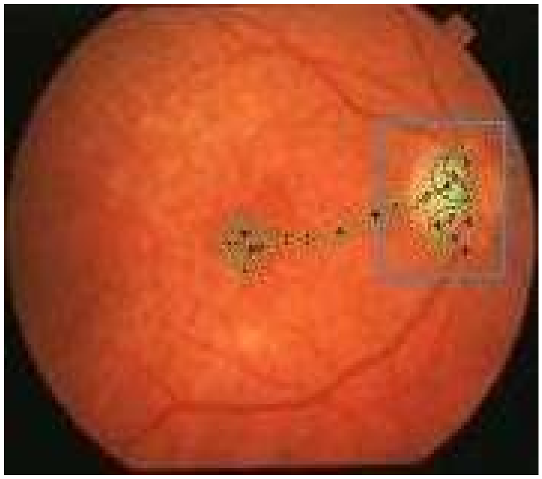

**Figure 4.1** Fixation sample image indicates the red dots. The fixation area is marked in green color.

The proposed method provides the maximum number of fixation list for $\text{EGFix}_{m,n}$( $X_i$ position, $Y_i$ position, duration). The fixations calculated for experts and non-experts are shown in Figures 4.2 (a) and (b), respectively.

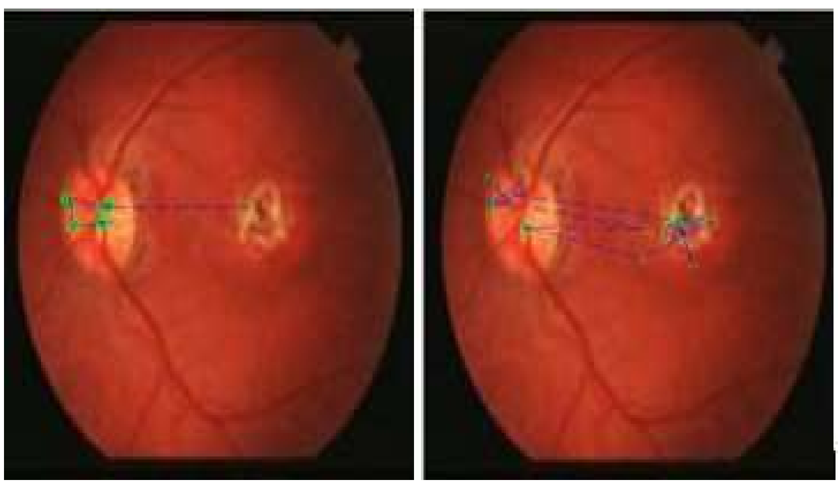

**Figure 4.2** (a) Indicated the OD region in the Expert group, and (b) Indicated the OD region in the non-expert group

To determine the total number of fixations, ROI duration, Dwells in ROI, Dwell time, and the number of fixations in ROI for the expert and non-expert. From that, the measurement e can plot the different features in the OD region. Different features are calculated, and these features can be plotted in figure 4.3.

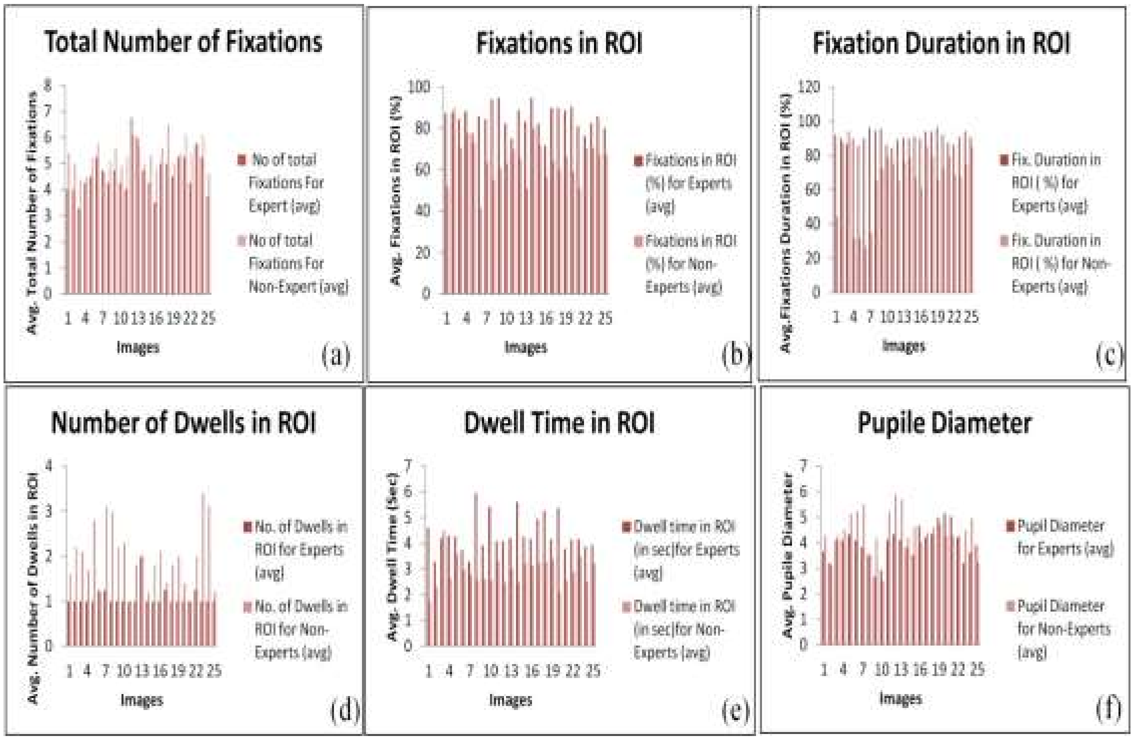


**Figure 4.3** (a) Total fixation, (b) ROI fixation, (c)ROI time duration, (d) dwells, (e) Time duration for dwell, (f) pupil diameter

Figure 4.4 represents the OD region for the heat map of the expert's gaze. This map fully focused on the region of the OD part of the eye. As well as calculated the same technique in the non-expert's region of the gaze. Finally, calculated different analysis such as gaze plot, focus plot, scan path, and heat map. Both experts and non-experts can analyze it with the help of Behavioral and Gaze Analysis (SMI BeGaze). BeGaze is a computing technique for the Detection of eye trackers.

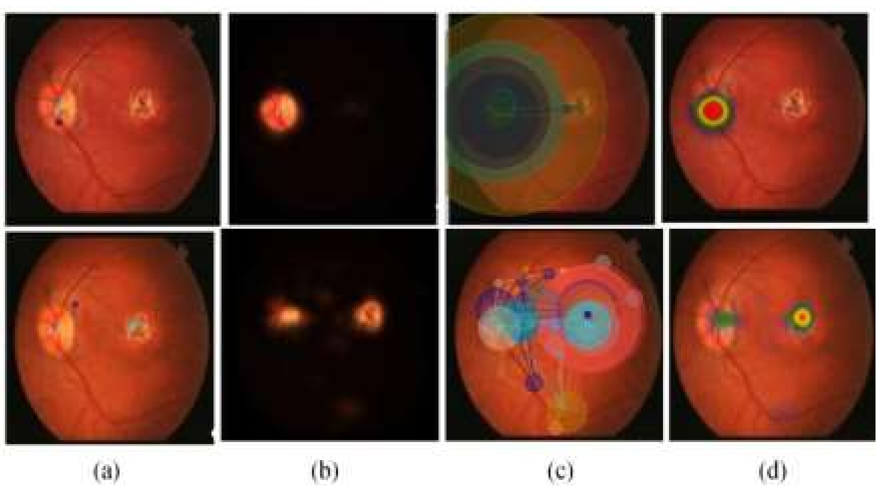


**Figure 4.4** Fixation dataset: (a) gaze image, (b) focus image, (c) scan path image, (d) heat map

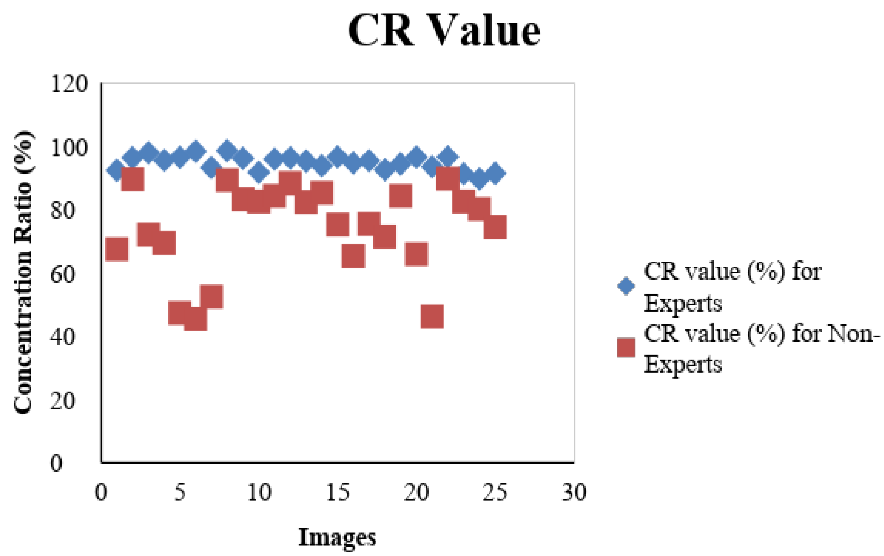


**Figure 4.5** Performance analysis of concentration ratio

**Table 4.1** Mean and standard deviation for expert and non-expert groups

| Features | Expert | | Non-expert | |
|---|---|---|---|---|
| | **Mean** | **Std. Deviation** | **Mean** | Std. Deviation |
| **Total fixation** | 4.604 | 0.79 | 4.99 | **0.50** |
| **ROI fixation (%)** | 85.11 | 6.04 | 61.08 | **16.07** |
| **Time duration** | 90.1 | 3.38 | 66.68 | **18.77** |
| **Total dwells** | 1.04 | 0.199 | 1.97 | **0.69** |
| **Duration of Dwell** | 4.37 | 0.66 | 2.91 | **0.55** |
| **Diameter** | **3.87** | **0.599** | **4.46** | **0.80** |

The expert and non-expert groups revealed differences in the mean test (Table 4.1): *t* critical two-tailed value is 2.0638.

**Table 4.2** Mean test for the expert and non-expert groups

| Feature | *t*-Stat value |
|---|---|
| **Total fixations** | **−6.15** |
| **ROI fixations** | **8.47** |
| **Time duration** | **6.20** |
| **Dwells** | **−6.29** |
| **Dwell time in ROI** | **7.65** |
| **Diameter** | **−2.87** |

From the table, the value gives the critical value of the region. Due to this problem, the null hypothesis is neglected and created another hypothesis. The confusion graph can be shown in figure 4.6.

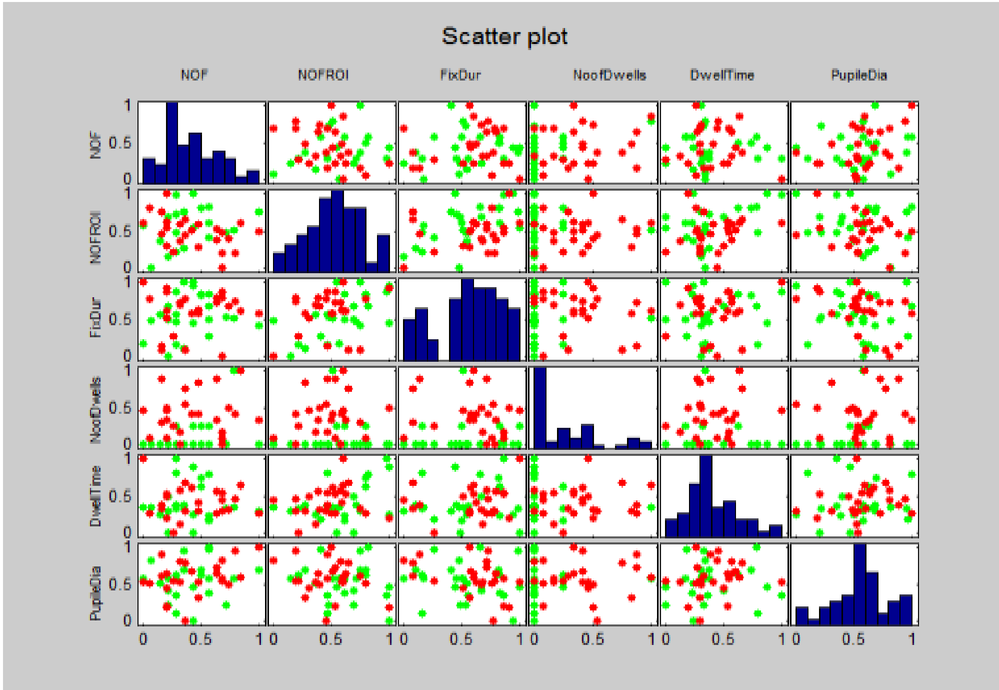


**Figure 4.6** Confusion graph for the Expert and Non-Expert features

## V. Conclusion

Several Computer-Aided Diagnosis (CAD) systems were developed for detecting glaucoma in its early stage using retinal images. The CAD systems mainly concentrate on identifying and detecting the nodules. There exist no CAD systems for identifying the stage of glaucoma. The major drawbacks of existing CAD systems are the accuracy in segmenting the nodule. Staging of the affected region at its investigation is the major predictor of survival, determining the treatment. In the 80-20 % testing phase, the training phase produces better accuracy (97.14 %) while comparing the other testing phase.

## References

[1] Sagar Honnungar, Sanyam Mehra & Samuel Joseph 2016, 'Diabetic Retinopathy Identification and Severity Classification,' CS229, FALL, pp. 1-5.

[2] SelvaraniGrace & Saranya, M., 2016' Fundus Image Screening for Diabetic Retinopathy' Indian Journal of Science and Technology, vol.9, no.25, pp.1-6.

[3] Rani, K. Vijila, and A. Alvin Ancy 2018, "Multiscale Image Enhancement Based on Natural Visual System." *Journal of Signal Processing* 4, no. 2.

[4] Shrutika A Patil & Manjiri Gogate 2017, 'Automatic Screening and Classification using Machine Analysis Technique,' International Conference On Emanations in Modern Technology and Engineering (ICEMTE-2017) ISSN: 2321-8169, vol. 5, no. 3.

[5] Srinivasan, C, Suneel Dubey & Ganeshbabu TR 2016, 'Complex Texture Features for Glaucomatous Image Classification System using Fundus Images,' International Journal of Engineering Research & Science (IJOER), vol. 2, no. 12, pp.106-113.

[6] Weiwei Gao & Jing Zuo 2016, 'Automated Detection of Hard Exudates in Fundus Images Using Improved Otsu Thresholding And SVM,' International Journal of Computer Science & Engineering Survey (IJCSES), vol. 7, no.1, pp.1-11.

[7] Ragav Venkatesan, Paraa S Chandakkar &Baoxin Li2017,'MIRank-KNN: multiple-instance retrieval of clinically relevant diabetic retinopathy images international Journal of Medical Imaging, vol. 4, no.3.

[8] Zhang, B, Wu, X, Yo, J, Li, Q & Karray, F 2010, 'Detection of microaneurysms using multiscale correlation coefficients,' Pattern Recognition, vol. 43, no. 6, pp., 2237–2248.

[9] Amreen Taj, C, Annapoorna, M, Deepika, KH, Keerthi Kumari, BA & Kanimozhi, S 2017, 'Detection of Exudates in Retinal Images using Support Vector Machine,' International Research Journal of Engineering and Technology (IRJET), vol. 4, no. 5, pp., 1847-1852.

[10] Anitha Somasundari & Janardhana Prabhu 2013, 'Detection of Exudates for the Diagnosis of Diabetic

Retinopathy,' International Journal of Innovation and Applied Studies, vol. 3, no. 1, pp. 116-120.

[11] Antal, B & Hajdu, 2014, 'An ensemble-based system for microaneurysm detection and Diabetic Retinopathy grading,' IEEE Transactions on Biomedical Engineering, vol. 59, no. 6, pp., 1720–1726.

[12] Falguni Thakkar & Rajvi Parikh 2016, 'A Survey on Automatic Detection of Diabetic Retinopathy Exudates from Retinal Fundus Images,' International Journal of Advanced Research in Computer and Communication Engineering, vol. 5, no. 5, pp.775-778.

[13] Ganesh, S & Basha, AM 2015, 'Automated Detection of Diabetic Retinopathy using retinal optical images,' International Journal of Science, Technology & Management, vol. 4, no. 2, pp.136-144.

[14] Jagatheesh, C & Jenila, M 2015**, 'Automatic Detection and Classification of Diabetic Retinopathy Lesion Using Bag of Visual Words Model,'** International Journal of Scientific and Research Publications, vol. 5, no. 9, pp.1-7.

[15] Mookiah, MRK, Acharya, UR, Martis, RJ, Chua, CK, Lim, CM, Ng, EYK & Laude, A 2013, 'Evolutionary Algorithms Based Classifier Parameter Tuning for Automatic Diabetic Retinopathy Grading: A Hybrid Feature Extraction Approach,' Knowledge-Based Systems, Vol. 39, pp. 9-22.

[16] Prakash, NB, Hemalakshmi, GR & Stella Inba Mary, M 2016, 'Automated grading of Diabetic Retinopathy stages in fundus images using SVM classifier,' Journal of Chemical and Pharmaceutical Research, vol.8, no.1, pp.637-541.

[17] Jahiruzzaman, MD&Aowlad Hossain ABM,2015,'Detection and classification of diabetic Retinopathyusing k-means clustering and Fuzzy Logic', International Conference on Computer and information technology.

[18] Jaya, T, Dheeba, J & Albert Singh, N 2015, 'Detection of Hard Exudates in Colour Fundus Images using Fuzzy Support Vector Machine-based Expert System,' Digit Imaging, vol.28, no.6, pp.761-768.

[19] Malathi, K & Nedunchelian, R 2017, 'A recursive support vector machine (RSVM) algorithm to detect and classify Diabetic Retinopathy in fundus retina images". Biomedical Research, pp. 1-8.

[20] Monzurul Islam, Anh Dinh, V & Khan Wahid, A 2017, 'Automated Diabetic Retinopathy Detection Using Bag of Words Approach,' J. Biomedical Science and Engineering, vol.10, pp.86-96.